NUMERICAL ANALYSIS OF CRACK INITIATION AND PROPAGATION BEHAVIOR IN ALUMINUM MATRIX COMPOSITES

Hiroyuki Toda*, Toshiro Kobayashi* and Takashi Goda**

*Department of Production Systems Engineering, Toyohashi University of Technology, Hibarigaoka, Tempaku-cho, Toyohashi city, AICHI 441-8580, Japan.
**Graduate school, Toyohashi University of Technology.

bstract A fracture-mechanics based simulation of a crack propagating through discontinuously-nforced composites is presented. The calculation incorporates microcrack initiation and shielding nd/or anti-shielding effects caused by both microcracks and reinforcements. Energy-based mixed-ode crack propagation criteria are used to specify the conditions for the onset of crack propagation nd crack propagation direction. Shielding effect due to the existence of a rigid reinforcement ddenly vanishes with the cracking or debonding of the reinforcement. Thereby crack propagation rection abruptly changes due to the generation of an opposite anti-shielding effect caused by the istence of a microcrack. Such phenomenon makes crack path morphology in the composite very mplicated. Optimum crack propagation mechanism to improve the fracture toughness of uminum composites is clarified by considering the extension of a main crack interacting with a ngle reinforcement.

eywords: *composite material, crack propagation, microcracking, elastic interaction, deflection*

INTRODUCTION

The fracture and toughening processes in the discontinuously-reinforced composites can be tributed to several possible mechanisms which involve both intrinsic and extrinsic mechanisms. me of the often observed micromechanisms of crack initiation and propagation include icrocracking far ahead of a crack-tip due to reinforcement fracture and/or interfacial debonding, e extension of microcracks followed by incorporation with a main crack, and resultant crack flection. Especially, it is dominant in aluminum composites with discontinuous ceramics nforcements due to large deformation incompatibility between the two phases. In such composite stems, the bridging of crack surfaces by unbroken fibers and crack pinning mechanism are rare ents because almost no reinforcement may remain intact nor hold sizable shielding effect caused elastic incompatibility. Because of complex interactions among a main crack and thousands of icrocracks and remaining reinforcements in practical composites, no general interpretation has en presented for the tortuous crack path in the failure of composites in spite of the numerous perimental investigations.

In this paper, aforementioned fracture processes are modeled in terms of the fracture echanics. The effects of reinforcement shielding, microcrack shielding and the easiness of icrocracking (i.e. the mechanical properties of both a reinforcement and an interface) on fracture ughness and crack propagation resistance are analyzed. Crack propagation processes through rious composites are compared and characterized by a series of calculations.

METHOD

Procedural details

The model chosen for this research is two dimensional because of computational necessity, in hich an elastic reinforcement having high elastic modulus is embedded in a softer matrix. A main ack is placed 30 μm apart from the reinforcement in the direction parallel to an initial crack plane. n external load is assumed to be completely perpendicular to the initial direction of the main crack hich means the application of pure mode I far-field loading. Non-linear finite element analysis is

utilized to compute internal stresses within the reinforcement which arise from deformation incompatibility between the reinforcement and the matrix. Experimental support is shown in Ref. [2]for usage of HRR singurality [1] in the calculation of averaged stress and strain distribution around the crack-tip of a stationary and propagating crack. Then local axial stresses inside the reinforcement, σ_r, and normal or shear stresses acting on the interface, σ_i , are computed in order to model microcracking by the normal fracture of the reinforcement or interfacial debonding when the main crack comes closer to the reinforcement. Criteria for the microcrack initiation are expressed as follows;

$$\sigma_r \geqq \sigma_{rb} \qquad (1)$$

$$\sigma_i \geqq \sigma_{db} \qquad (2)$$

where σ_{rb} and σ_{db} are the fracture strength of a reinforcement and interfacial bonding strength respectively.

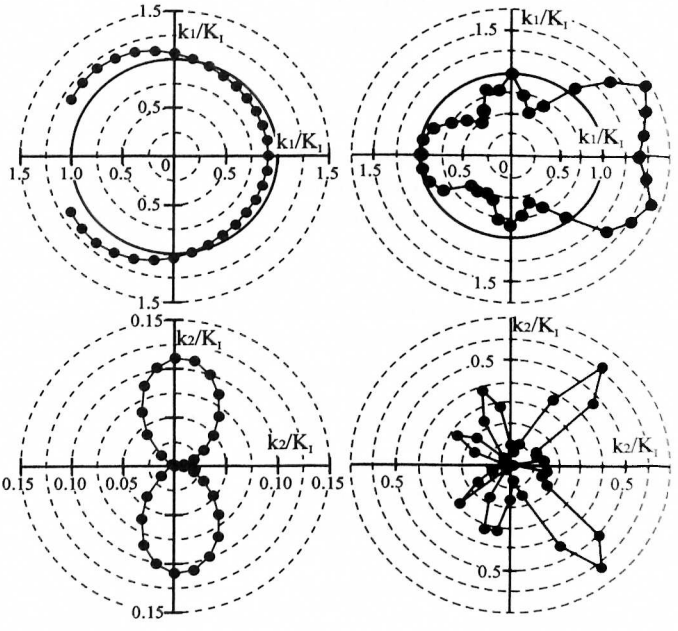

(a)Reinforcement shielding (b)Microcrack shielding

Fig.1 The variations of mode I and mode II stress intensity factors at the tip of a main crack as a function of the azimuth from the crack-tip. (a)shielding due to the existence of a rigid reinforcement, (b)microcrack shielding. An SiO2/Epoxy system is assumed.

The deformation incompatibility is also attributed to both shielding effect and the generation of mixed-mode stress states at the tip of a main crack in spite of the assumption of mode I remote loading. This mechanism arises primarily from load transfer from the matrix to the reinforcement. Another shielding mechanism also arises from the relaxation of matrix deformation due to the existence of a microcrack. The interaction effect of a microcrack on the local crack-tip stress intensity factors is estimated using the Gong and Horii's solution [3]. The comparison of the effects of the reinforcement shielding and the microcrack shielding is shown in Fig.1. The effect of the microcrack shielding is quite contrary to that of the reinforcement shielding. A microcrack ahead of a main crack increases the local stress intensity factor in the mode I direction at the tip of the main crack significantly (i.e. so-called anti-shielding or amplification effect), while an undamaged reinforcement ahead of the main crack slightly decreases it (i.e. shielding effect). Both effects are accompanied by the generation of local mode II crack driving force, k_{II}, which gives rise to the deflection of the main crack. But the signs of generated k_{II} are opposite, thereby both phenomena makes the main crack deflected in the reverse direction.

To simulate the onset of crack propagation and subsequent stable crack propagation under the mixed-mode loading condition, maximum energy release rate criterion[4] and minimum strain energy density factor criterion[5] are adopted. The minimum strain energy density factor, S, criterion whose validity has been confirmed for the ductile fracture of 5000 series aluminum alloys [5], is utilized for aluminum matrix composites, while the maximum energy release rate, G, criterion is utilized for brittle solid matrix composites. The criteria for crack initiation are given in eq. (3), and the equations which give the crack propagation direction, β, are given in eq. (4).

$$S \geqq S_c \quad \text{or} \quad G \geqq G_c \quad \text{for } \theta = \beta \tag{3}$$

$$\partial S / \partial \theta = 0 \quad \text{or} \quad \partial G / \partial \theta = 0 \quad \text{at which } \theta = \beta \tag{4}$$

In eq. (3), S_c and G_c are material constants representing crack initiation toughness which corresponds to K_{IC} or J_{IC} under the pure mode I stress state.

Recently, Rubinstein analyzed the material toughening mechanism based on the crack-path deflection[6]. According to him, the effect basically depends on the last curved segment, so the analysis of only the last curved segment is sufficient to describe the shielding effect. Variation of k_I due to the existence of intermediate deflected segments is at most 0.96% in his calculation. Therefore, in this analysis, only the effect of the last deflected segment is calculated using Bilby's solution[7].

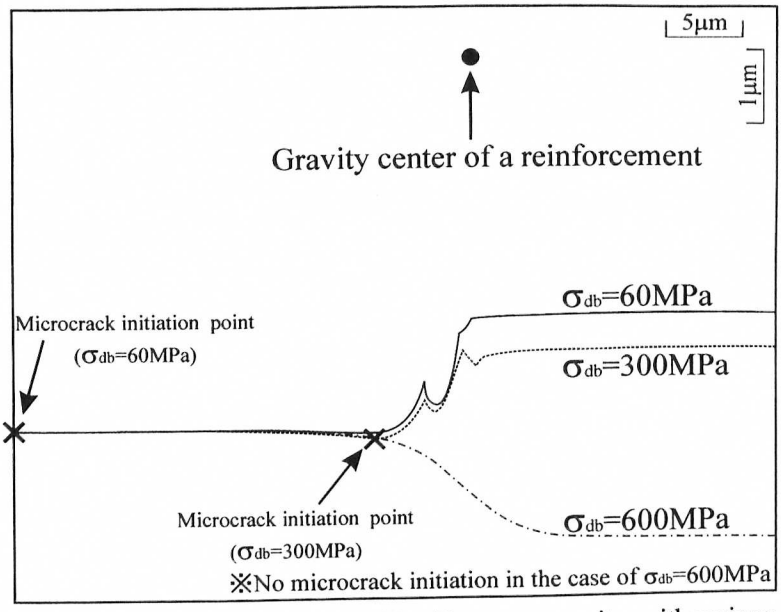

Fig.2 Crack path predictions for SiO_2p/Epoxy composites with various interfacial bonding strength.

$$k_I = a_{11}(\theta)K_I^0 + a_{12}(\theta)K_{II}^0 \tag{5}$$

$$k_{II} = a_{21}(\theta)K_I^0 + a_{22}(\theta)K_{II}^0 \tag{6}$$

where K_I^0 and K_{II}^0 are the far field stress intensity factors and θ is a deflection angle. The other details of calculation method are available in the previous paper of the series of this research [1]. The essential sequence of the calculations is presented as a flow chart in Fig.6 of Ref. [1].

Table 1 Material properties.

		SiCp/Al	SiO_2p/Epoxy
Matrix	Fracture toughness	29.4MPa$\sqrt{m}$	1.12MPa$\sqrt{m}$
	Proof stress	249.7MPa	———
	Work hardening rate	4.2	———
	Young's Modulus	70.8GPa	3.1GPa
	Poisson ratio	0.33	0.31
Reinforcement	Diameter	5μm	5μm
	Strength	3～21GPa	3GPa
	Young's Modulus	580GPa	70GPa
	Poisson ratio	0.19	0.26
Interface	Bonding strength	1690MPa	60～600MPa

2.2 Model composites

Fracture characteristics of an SiC particle reinforced A6061 aluminum alloy are analyzed in comparison to an SiO_2 particle reinforced epoxy composite in which the deformation incompatibility of the two phases is more remarkable than in the aluminum composite. Mechanical properties of the composites are listed in Table 1. The initial location of the tip of a main crack is at a x coordinate of –30μm and a y coordinate of –5μm with the center of a square reinforcement as its origin. The other details of the properties are described elsewhere [4].

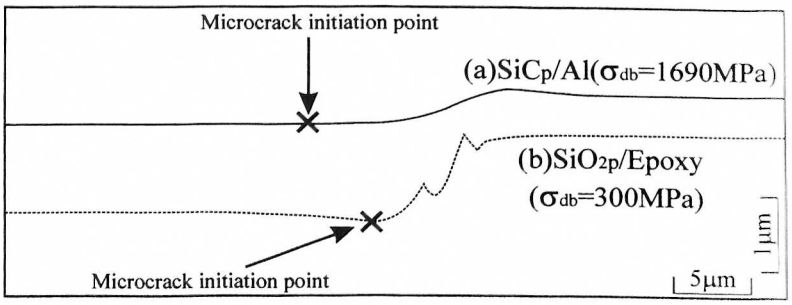

Fig.3 Comparison of the predicted crack path morphologies between the SiCp/Al and SiO2p/Epoxy composites.

3. RESULTS AND DISCUSSION

The comparison of predicted crack paths when a main crack passes by a single reinforcement with the different levels of interfacial bonding strength is shown in Fig.2. Microcracks were initiated at reinforcement/matrix interfaces due to interfacial debonding in two of the three cases, while no microcracking is predicted in the remaining case. In Fig.2 (a), low interfacial strength, i.e. $\sigma_{d\,b}$ = 60MPa, is assumed which has been reported experimentally in the literature [8]. Since the value is as low as the overall applied stress, a microcrack is initiated easily far ahead of the crack-tip. Then the main crack is strongly attracted toward the microcrack, thereby the main crack considerably deflected. For the case of $\sigma_{d\,b}$ = 300MPa, a microcrack is initiated when a main crack is passing alongside of the reinforcement as shown in Fig.2 (b). Before the microcrack initiation, the main crack slightly deflects from the reinforcement. However, after microcrack initiation, the crack seems to be attracted into the reinforcement. The crack path morphologies after the microcrack initiation are quite similar, and it is self-evident because the local k_I and k_{II} at the tip of a main crack are merely affected by the microcrack shielding in this calculation, which is dependent only on the location and length of a microcrack . When the interfacial bonding strength is as high as 600MPa, no microcracking occurs and the main crack deflects monotonously as if it escaped from the reinforcement due to the reinforcement shielding effect. Note that the crack never approaches the reinforcement.

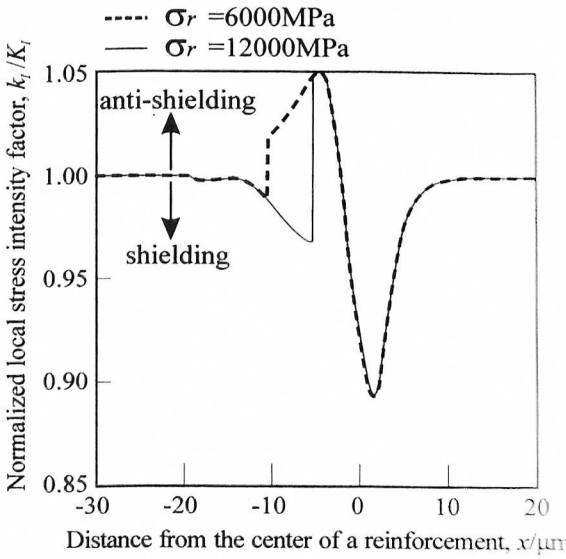

Fig.4 Variations of k_I with the extension of a main crack.

Figure 3 shows the same crack path prediction for the SiCp/A6061 aluminum alloy composite together with the result for the polymer matrix composite shown in Fig.2 (b). The amount of crack deflection in the aluminum composite is small in comparison to the SiO_2/Epoxy system. Since the

compatibility of the Al/SiC interfaces is superior which is reflected in the reported high interfacial bonding strength value, microcracking is almost always caused by the breakage of a reinforcement in the Al/SiC systems. In the case of the polymer matrix composite, the interfacial debonding occurs at the nearest interface to the tip of a main crack, so the distance between the microcrack initiation point and the crack-tip is different in both of the systems even when the locations of microcrack initiation are similar. It results in conspicuous difference in the predicted crack paths.

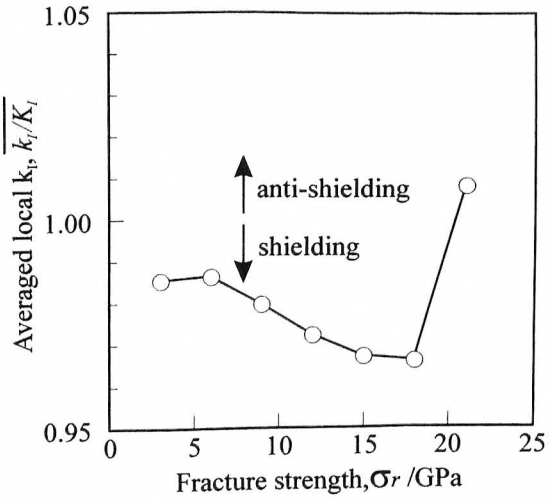

Fig.5 Effect of the fracture strength of a reinforcement on the local driving force of a main crack, representing the existence of an optimum strength value for the crack propagation resistance.

Figure 4 shows variations of local crack driving forces, k_I, with the extension of the main crack for two different levels of reinforcement strength. Microcracking occurs at an approximate x coordinates of –10.4μm with the reinforcement center as its origin for the case of σ_r = 6000MPa, while it is –5.2 μm for σ_r = 12000MPa. k_I decreases slightly before the microcrack initiation as the crack-tip approaches the reinforcement due to the constraint of crack-tip deformation by the reinforcement. k_I increases drastically at the same time the microcracking occurs, which is attributed that the shielding effect due to the reinforcement is replaced by the anti-shielding effect due to the existence of a microcrack. As shown in Fig.1, the effects of both mechanisms are completely opposite both for k_I and k_{II}, and the effect of the microcrack shielding is much effective than another. Subsequently, the anti-shielding effect from the microcrack is reversed to shielding effect when the microcrack is located behind the crack-tip. Therefore, the crack extension is effectively retarded in this vicinity. When the reinforcement strength is as high as 12000MPa, antishielding occurs only in a tiny segment of the crack path directly under the reinforcement center. Therefore, even the microcrack predominantly exerts shielding effect in this case. We would, therefore, infer that such retardation of microcracking when the main crack approaches the reinforcement can improve overall crack propagation resistance of the discontinuously-reinforced composites.

In order to evaluate the effect of the reinforcement strength on the toughening behavior of the aluminum matrix composite, local mode I stress intensity factor at the tip of the main crack is averaged between the x coordinates of –10 and 10 μm with the reinforcement as a center. It is plotted as a function of the reinforcement strength as shown in Fig. 5. When the reinforcement strength is higher than 18600MPa, no microcracking occurs with the extension of a main crack. Higher reinforcement strength delays microcracking gradually until it reaches 18600MPa, and simultaneously suppresses the baneful effect of the microcrack anti-shielding. When the reinforcement strength is higher than 18600MPa, only the reinforcement shielding affects the crack propagation through the composite. Since the antishielding effect when the reinforcement is located behind the crack-tip is greater than the shielding effect when it is ahead of the crack-tip, averaged k_I becomes larger than K_I which means antishielding effect on the average. 18600MPa is concluded as an optimum value to obtain high toughness and it brings 3% overall increase in the toughness of the aluminum composite by estimating the effect of only a single reinforcement.

In these calculations, microcracking phenomenon is taken to mean substantially that the reinforcement is removed from the model with the cracking. However, actually, broken

reinforcement or a reinforcement with a debonded interface should hold some mechanical effects especially in the direction perpendicular to the microcrack. Therefore, the calculation in Fig.5 involves some overestimation that the microcrack shielding is not compensated by the reinforcement shielding to some extent when the reinforcement strength is below 18600MPa. Nevertheless, the trends obtained in a series of the calculations suggest helpful information for the control of engineered microstructures. The major limitations of the model include the two dimensional nature of the solution. However, the solution can be extended to models considering plural reinforcements like ordinary practical materials in future.

4. CONCLUSIONS

(1) Microcracks initiated ahead of a main crack exert anti-shielding effect which corresponds to overall toughness degradation. While rigid reinforcements without any damage bring shielding effect which enhances the toughness of composites. Subsequently, when the tip of a main crack passes by the reinforcement or the microcrack, the effects just reverse suddenly. The degree of reinforcement shielding in aluminum matrix composites is much smaller than that in polymer matrix composites.

(2) The most preferable sequence of crack propagation for toughening is 1) the generation of strong shielding effect due to the reinforcement with high elastic modulus, 2) microcracking when distance between the reinforcement and the main crack is the closest. Thereby anti-shielding effect due to the microcracks which exist ahead of the main crack is effectively suppressed and only the preferable effects of the microcrack shielding and the reinforcement shielding can be utilized for toughening.

(3) Since the interfacial bonding strength is sufficiently high in the case of an Al /SiC system, the predominant factor for toughening is the fracture strength of reinforcements. The existence of an extremum in the fracture strength of reinforcements is predicted, which maximizes crack propagation resistance. It is estimated as 18600MPa for the model composite.

REFERENCES

[1]H.Toda and T.Kobayashi, Metall. Mater. Trans. A, 28A(1997), 2149.
[2] J.R.Rice and G.F.Rosengren: J. Mech. Phys. Solids, 16(1968), 1.
[3]S.X.Gong and H.Horii: J. Mech. Phys. Solids, 37(1989), 27.
[4]B.Cotterell: Int. J. Fract., 1(1965), 96.
[5]G.C.Sih: Int. J. Fract., 10(1974), 305.
[6] A.A.Rubinstein: J. Appl. Mech., 57(1990), 97.
[7] B.A.Bilby, G.E.Cardew and I.C.Howard: Fracture 1977, vol.3, Ed. by D.M.R.Taplin, Univ. of Waterloo Press, (1977), 197.
[8]T.M.Mower and A.S.Argon: Polym. Mater. Sci. Eng., 70(1994), 204.